Electronic Supplementary Information for Dalton Transactions

Supporting Information for:

A Homologous Heterospin Series of Mononuclear Lanthanide/$TCNQF_4$ Organic Radical Complexes

Nazario Lopez,[a] Hanhua Zhao,[a] Andrey V. Prosvirin,[a] Wolfgang Wernsdorfer[b] and Kim R. Dunbar[a*]

[a] Department of Chemistry, Texas A&M University, College Station, TX 77842 (USA). Fax: (+1) 979-845-7177; Tel: (+1) 979-845-5235. e-mail: dunbar@mail.chem.tamu.edu
[b] Institut Néel, CNRS & Université J. Fourier, BP-166, Grenoble, Cedex 9 (France)

Contents:

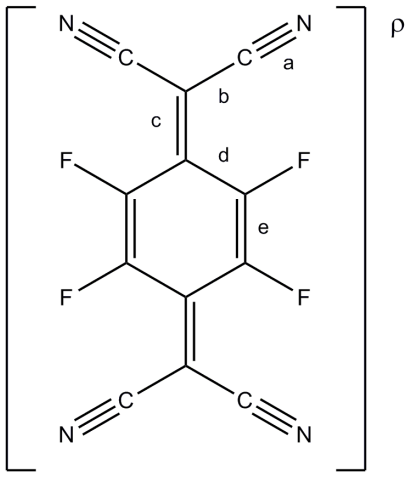

Scheme S1. Schematic drawing of $TCNQF_4$. The bond lengths used in the Kistenmacher relationship are labeled with the corresponding lower case letters.

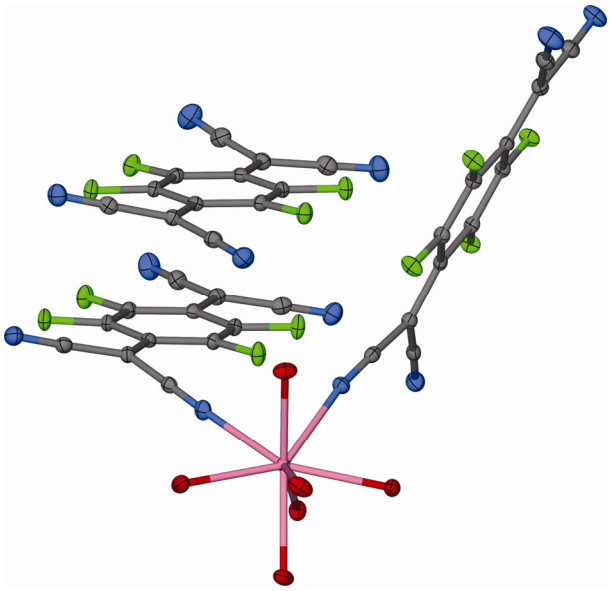

Figure S1. Color version of Figure 1. Molecular structure of the cationic complex along with the uncoordinated $TCNQF_4$ molecule in **Ho**. Interstitial water molecules and hydrogen atoms have been omitted for the sake of clarity. Ho = pink, O = red, N = blue, C = gray F = green.

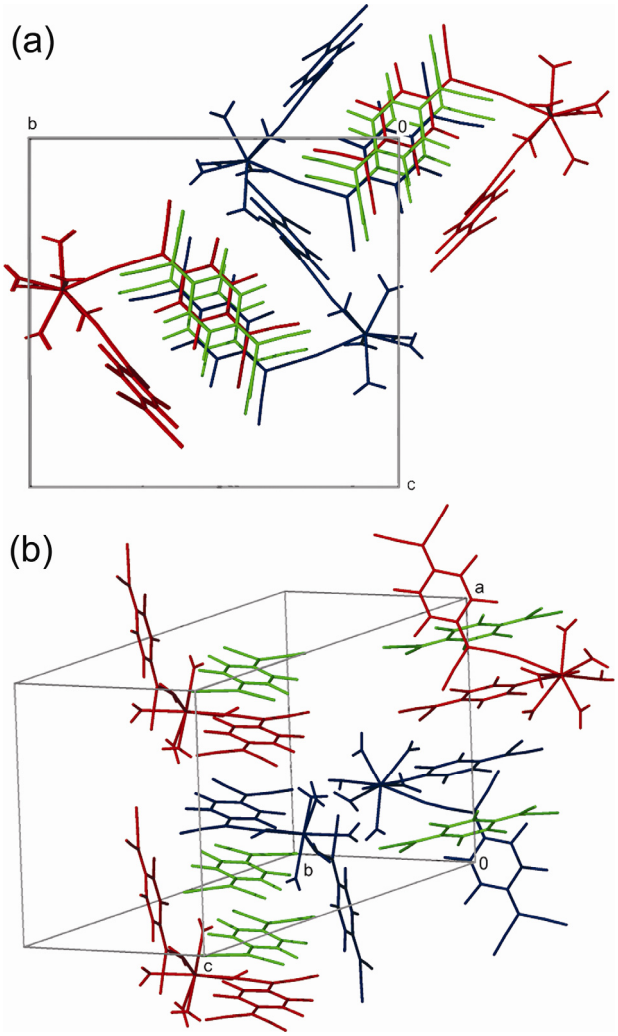

Figure S2. Color version of figure 2. Packing diagrams of the **Ho** compound (a) viewed along the *a* axis and (b) depicting □–□ stacking interactions in the crystal structure of **Ho**. The interstitial water molecules are omitted for the sake of clarity. Blue = the cationic complex $[Ho(TCNQF_4)_2(H_2O)_6]^+$, which has the unstacked $TCNQF_4$ moiety pointing down; red = the cationic complex $[Ho(TCNQF_4)_2(H_2O)_6]^+$, for which the unstacked $TCNQF_4$ unit is pointing up; green = uncoordinated $TCNQF_4$ molecules.

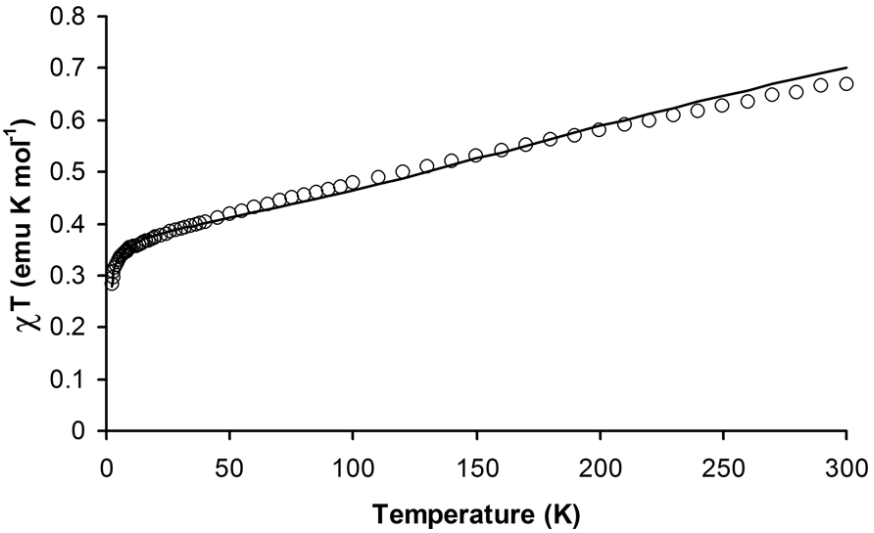

Figure S3. Temperature dependence of the χT product for **La**. The solid line is the best fit to a Heisenberg chain model with the Hamiltonian $H = -2J\Sigma S_i S_{i-1}$, and parameters: J = -140 cm^{-1}, g = 2.00.

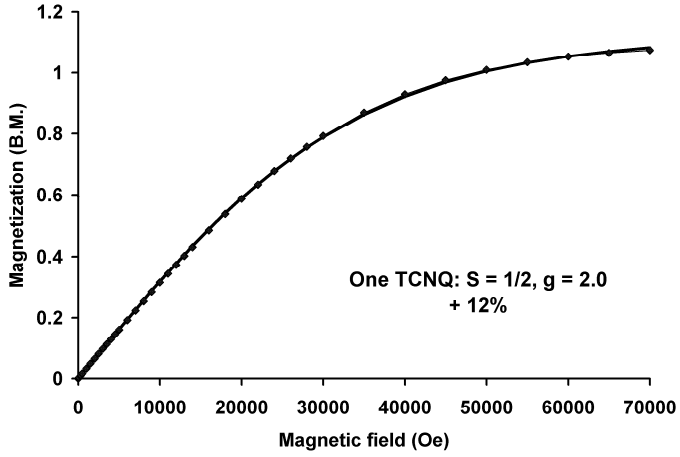

Figure S4. The field dependent magnetization of the **La** complex at 1.8 K, in the range of 0-7 T. The solid line is the Brillouin function fit with parameters of 1.12 S = ½ and g = 2.0.

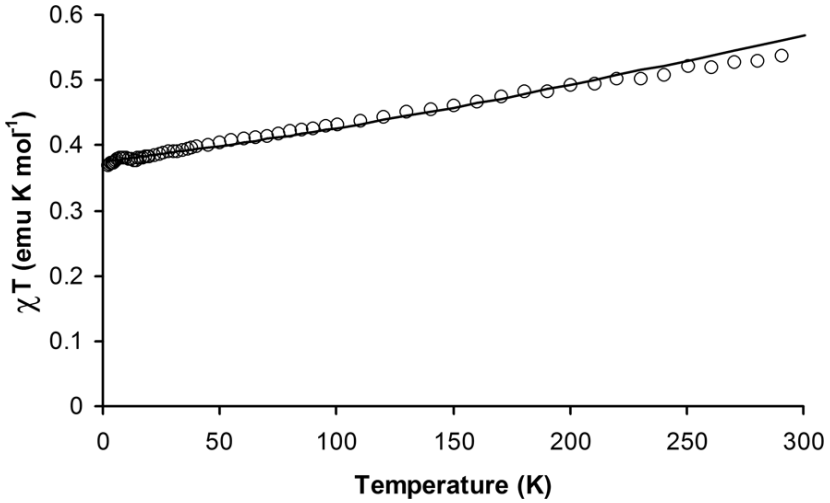

Figure S5. Temperature dependence of the χT product for **Y**. The solid line is the best fit to a Heisenberg chain model with the Hamiltonian $H = -2J\Sigma S_i S_{i-1}$, and parameters: J = -230 cm^{-1}, g = 2.00.

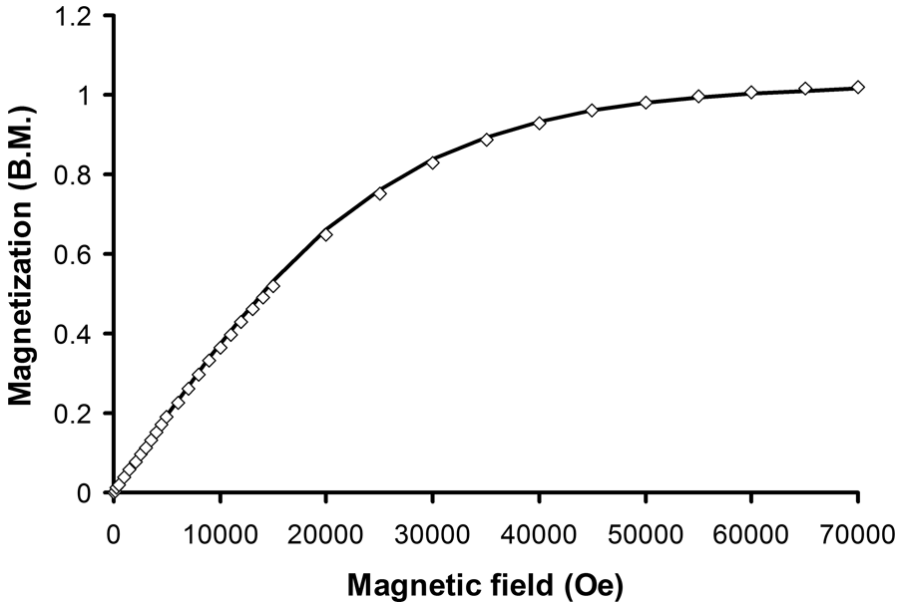

Figure S6. The field dependent magnetization of the **Y** complex at 1.8 K, in the range of 0-7 T. The solid line is the Brillouin function fit with parameters S = ½ and g = 2.05.

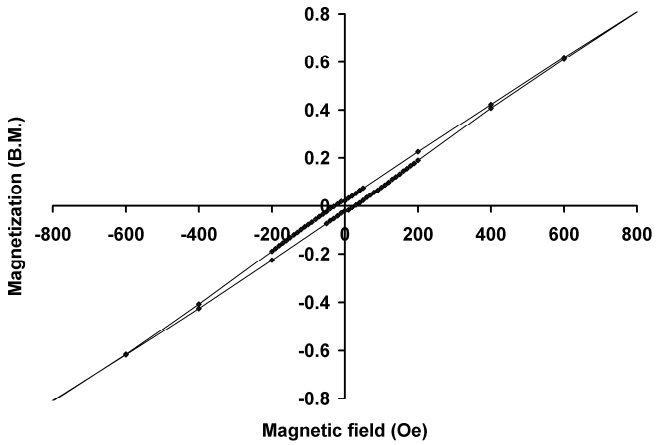

Figure S7. Hysteresis loop for the **Dy** complex.

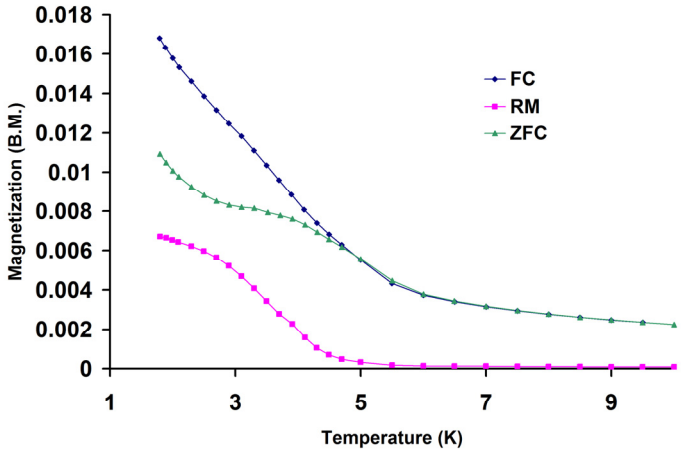

Figure S8. Field-cooled (FC), zero-field-cooled (ZFC) and remanent magnetization (RM) of the **Dy** complex.

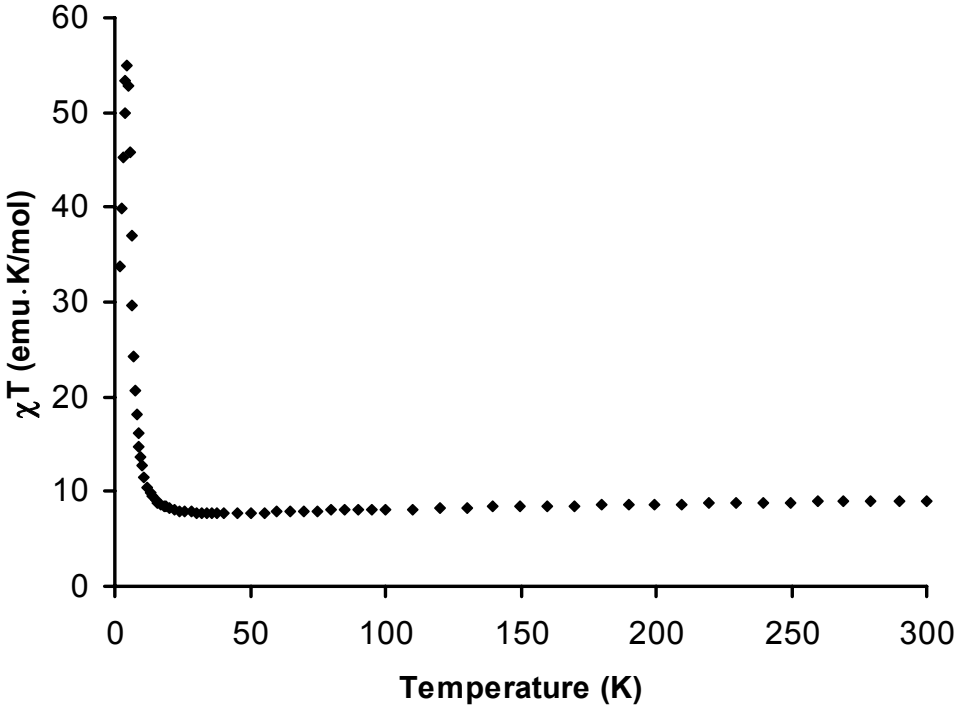

Figure S9. Temperature dependence of the χT product for dehydrated **Gd**.

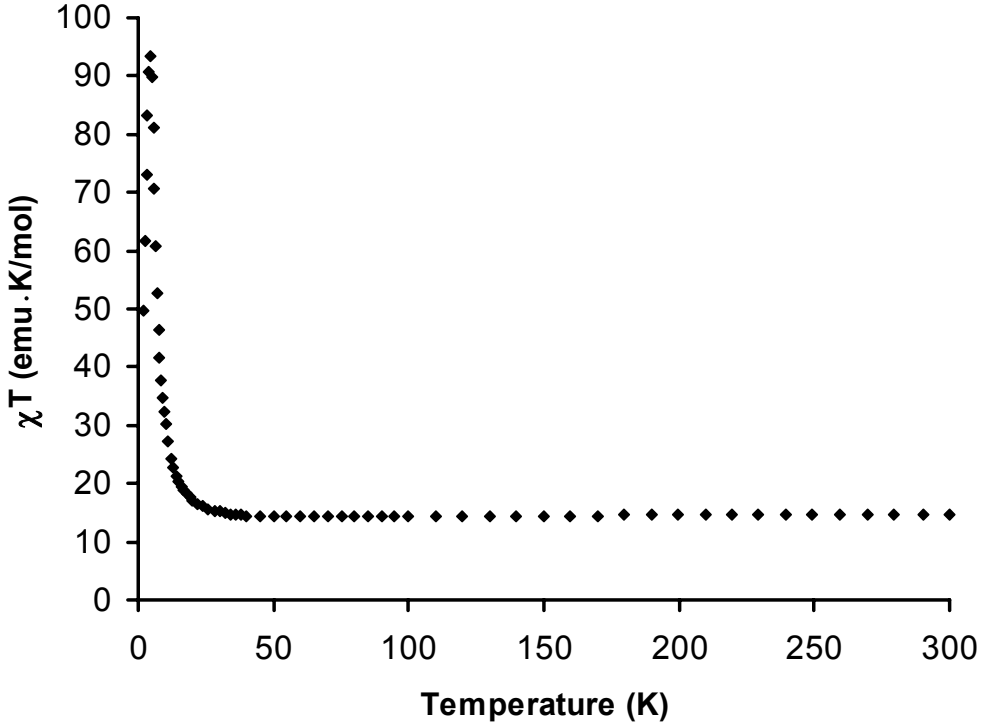

Figure S10. Temperature dependence of the χT product for dehydrated **Dy**.

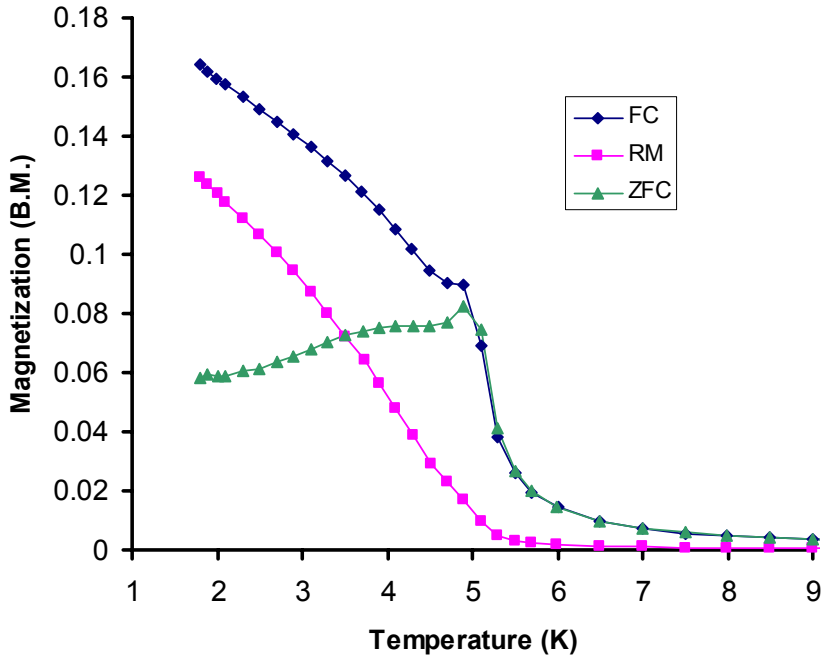

Figure S11. Field-cooled (FC), zero-field-cooled (ZFC) and remanent magnetization (RM) of dehydrated **Gd**.

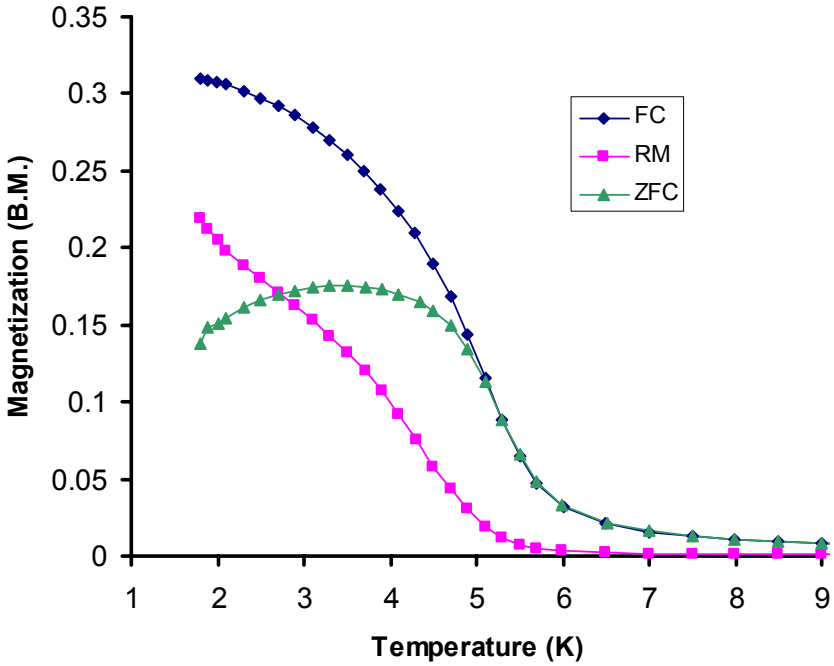

Figure S12. Field-cooled (FC), zero-field-cooled (ZFC) and remanent magnetization (RM) of dehydrated **Dy**.

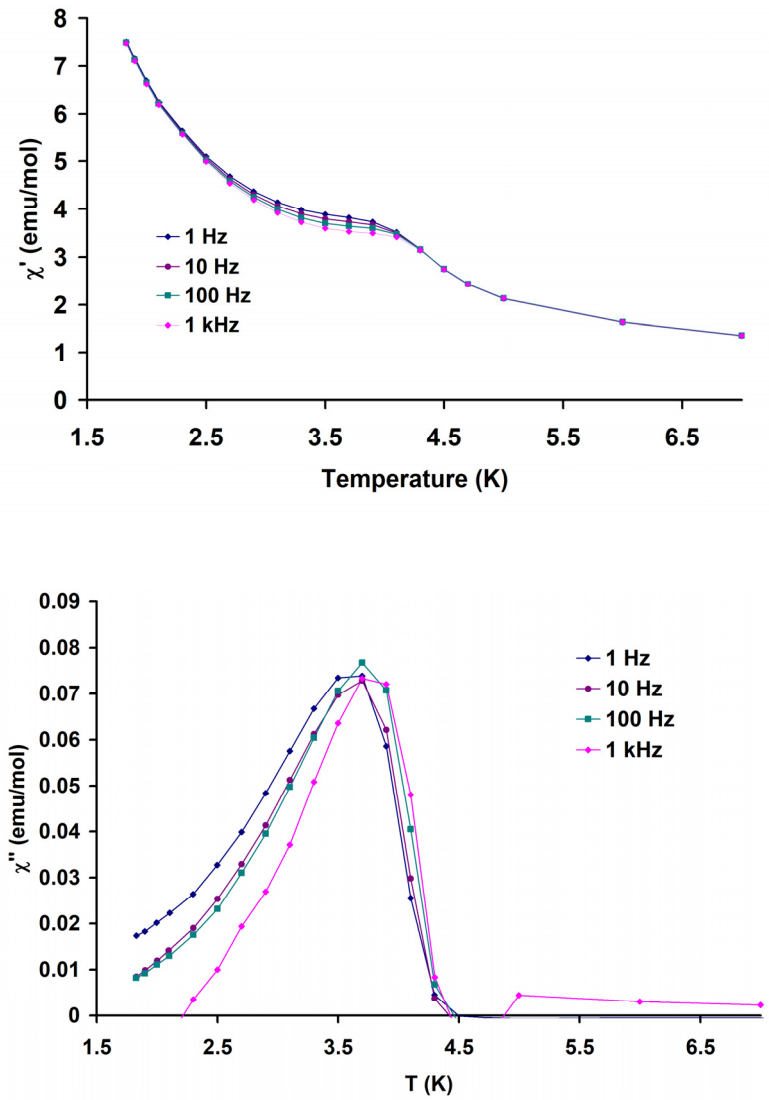

Figure S13. Temperature dependence of the real χ' and imaginary χ'' components of the AC magnetic susceptibility of the **Gd** complex measured in an oscillating field of 3 Oe at different frequencies.

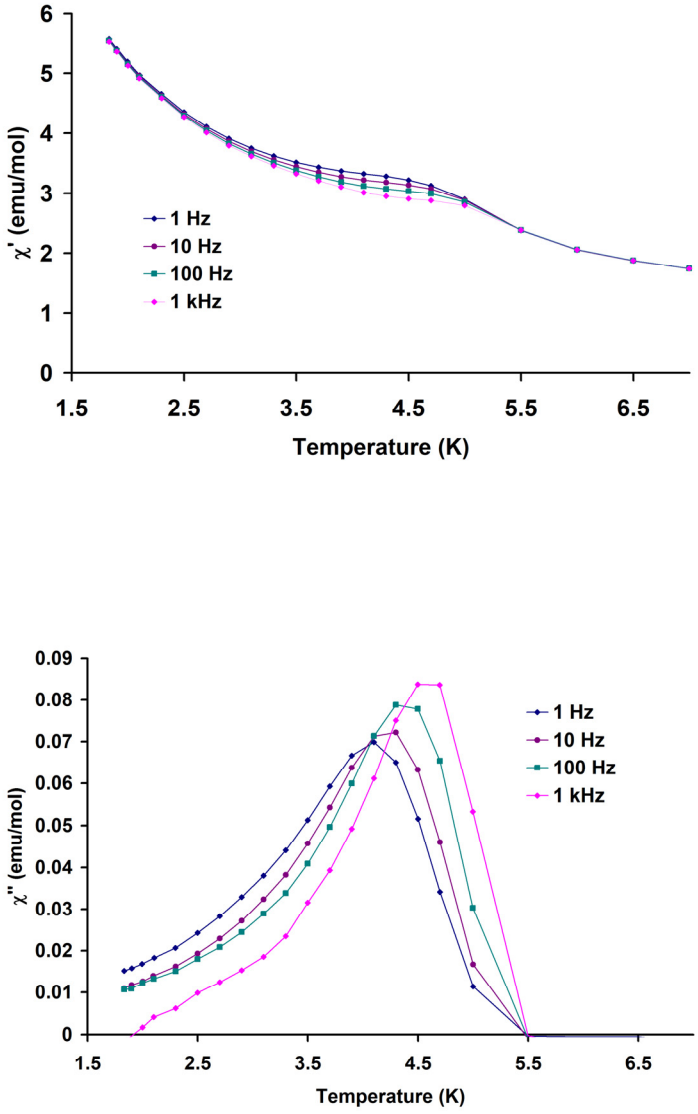

Figure S14. Temperature dependence of the real χ' and imaginary χ'' components of the AC magnetic susceptibility of the **Dy** complex measured in an oscillating field of 3 Oe at different frequencies.

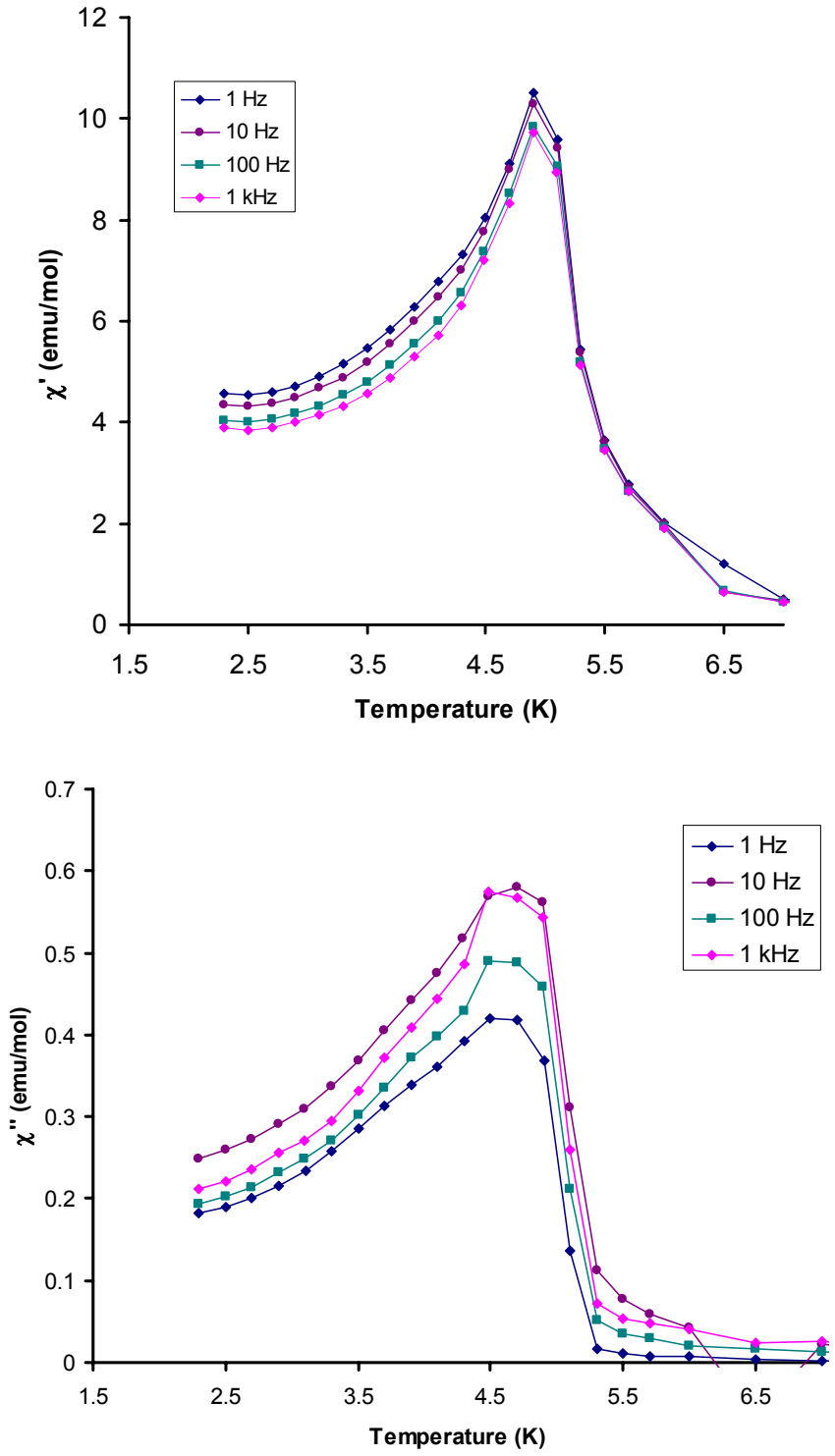

Figure S15. Temperature dependence of the real χ' and imaginary χ'' components of the AC magnetic susceptibility of the dehydrated **Gd** compound measured in an oscillating field of 3 Oe at different frequencies.

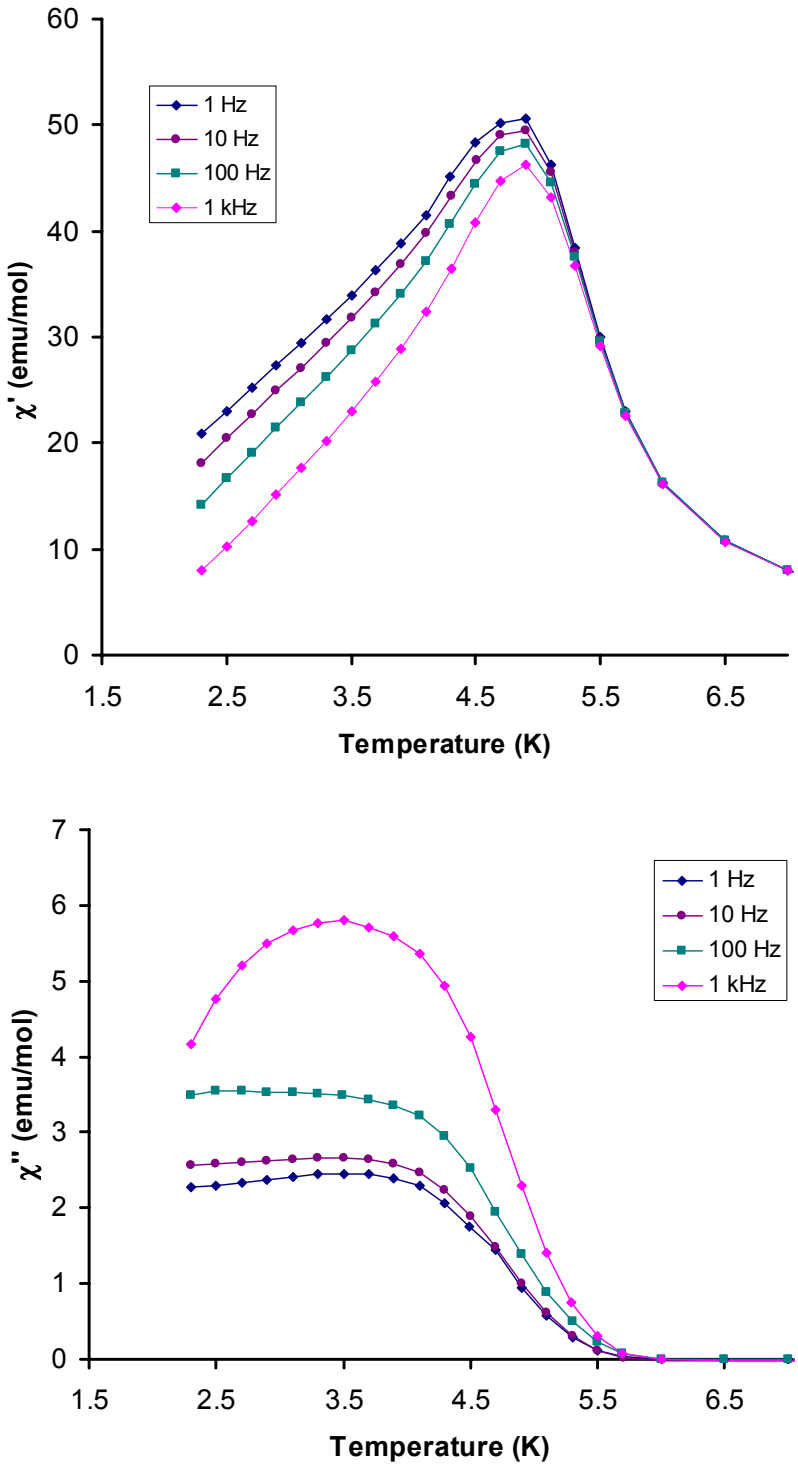

Figure S16. Temperature dependence of the real χ' and imaginary χ'' components of the AC magnetic susceptibility of the dehydrated **Dy** compound measured in an oscillating field of 3 Oe at different frequencies.

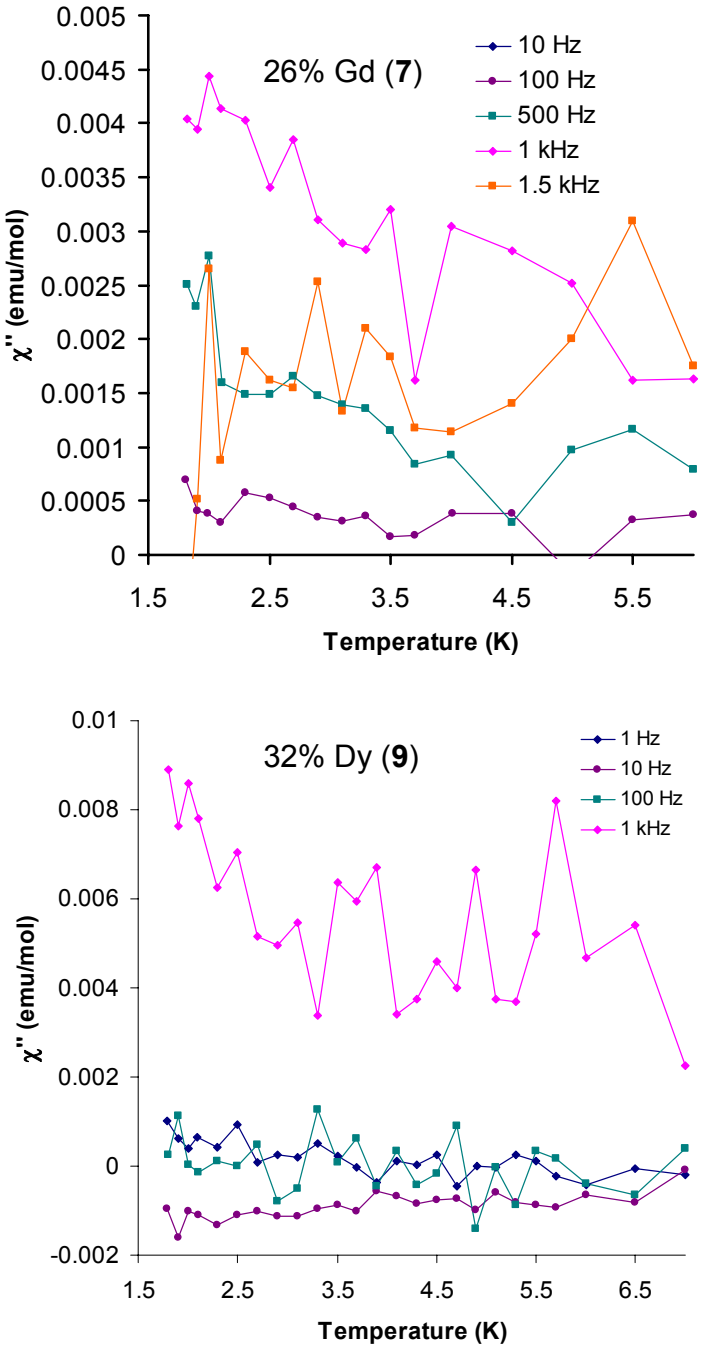

Figure S17. Temperature dependence of the imaginary χ'' component of the AC magnetic susceptibility for compounds **7** (top) and **9** (bottom) measured in an oscillating field of 5 Oe at zero applied magnetic field.

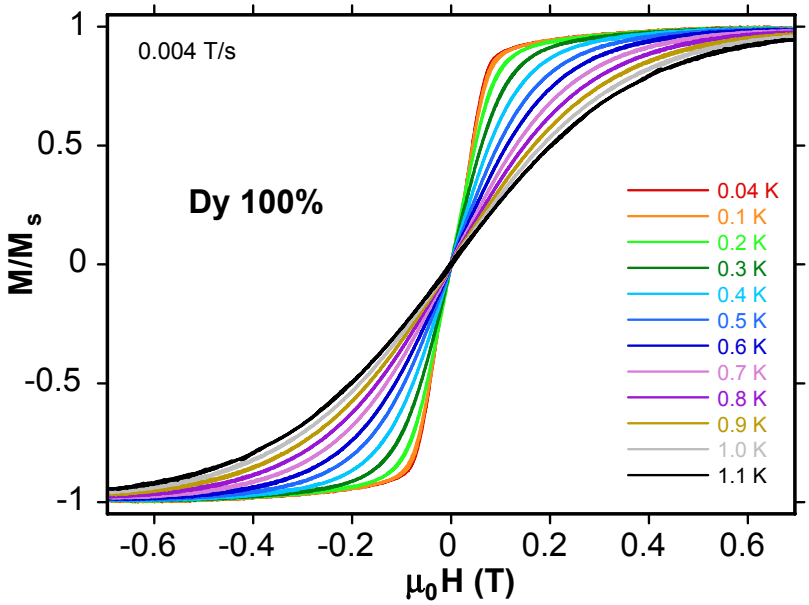

Figure S18. Micro-SQUID magnetization scans collected for **Dy** at temperatures from 0.04 K to 1.1 K at 0.004 T/s. Magnetization values are normalized to the magnetization value at 1.0 T.

Table S1. Hydrogen-bond distances for **Ho**

D—H ···A	D—H (Å)	H ···A (Å)	D ···A (Å)	D—H ···A (°)
O1—H1A ··· N9	0.80(3)	2.04(5)	2.84(8)	171(8)
O1—H1B ··· O1S	0.81(3)	1.96(8)	2.78(1)	171(0)
O3—H3A ··· O2S	0.80(3)	1.87(8)	2.68(1)	169(7)
O4—H4A ··· O3S	0.87(3)	1.87(2)	2..75(5)	166(0)
O1S—H1SA···O2S	0.83(3)	2.12(6)	2.95(9)	153(7)

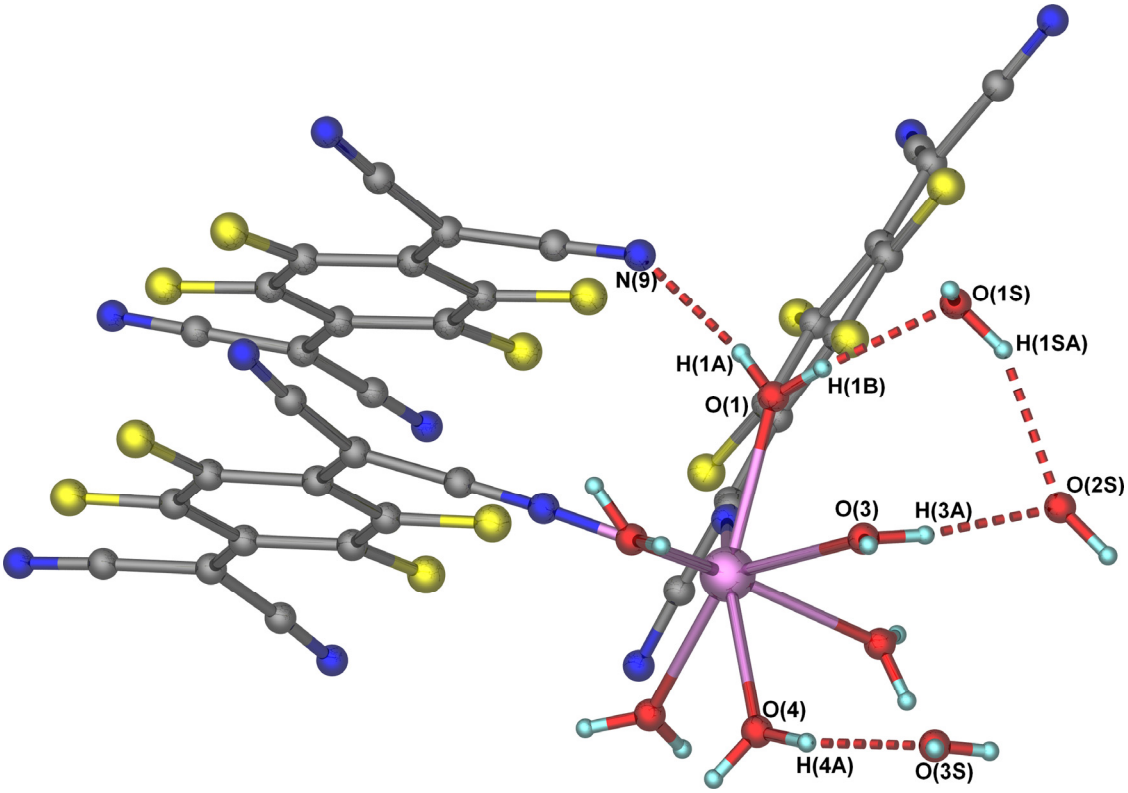

Figure S19. View of the hydrogen bond interactions in the **Ho** complex. Ho = pink, O = red, N = blue, C = gray, F = yellow, H = light blue.